VIP Bioinorganic Chemistry

DOI: 10.1002/anie.201108360

Photodynamic Effect in Near-IR Light by a Photocytotoxic Iron(III) Cellular Imaging Agent**

Uttara Basu, Imran Khan, Akhtar Hussain, Paturu Kondaiah, and Akhil R. Chakravarty**

Realization of a metal-based photocytotoxic agent in near-IR light is, so far, an elusive goal in photodynamic therapy (PDT) of cancer.[1–4] PDT is a non-invasive mode of therapeutic treatment of cancer, in which selective light activation of a photosensitizer within the tumor damages the cancer cells and leaves unexposed healthy cells unaffected.[5] Photofrin and its analogues, phthalocyanines, and lutetium(III) texaphyrin (LUTRIN) are few clinically tested PDT agents.[5–7] Photofrin, upon photoactivation in red light (633 nm), generates singlet oxygen by energy transfer by a type II pathway.[8,9] Deficiencies that are associated with such organic molecules are prolonged skin sensitivity and hepatotoxicity, which limits their therapeutic potential.[10] Moreover, the efficacy of an organic PDT agent depends largely on its ability to generate singlet oxygen in the cancer cells. To circumvent these drawbacks, biocompatible transition-metal complexes with their versatile coordination geometry, as well as varied spectral and redox properties, could be suitably designed as potent PDT agents. The redox active complexes could provide photoredox as an alternate pathway for cellular damage. Sustained efforts have yielded a variety of ruthenium, rhodium, platinum, and 3d metal-based complexes that are photocytotoxic under visible light with varied success.[11–17]

The basic requirement of PDT is a photosensitizer that can be activated in near-IR light to allow greater tissue penetration.[5] Copper(II) and oxidovanadium(IV) complexes have metal-centered absorption bands above 600 nm.[17] The major drawback of the copper(II) complexes is their high, thiol-induced, dark cellular cytotoxicity, which is absolutely undesirable in PDT.[17a,18] Oxidovanadium(IV) complexes have low dark cytotoxicity, but their low intensity d–d band near 700 nm and low molar extinction coefficient (ε) values make them ineffective as near-IR light photosensitizers.[17b] To surmount these shortcomings, we have tailored and successfully synthesized a ternary iron(III) complex that has a dipicolylamine ligand with a pendant anthracenyl moiety as a photosensitizer-cum-DNA binder, a catecholate ligand to obtain an intense ligand-to-metal charge-transfer (LMCT) band within the near-IR PDT spectral window (620–850 nm), and iron as a bioessential metal to reduce the metal-induced cellular toxicity. Herein, we present a structurally characterized iron-based PDT agent which targets the nuclear DNA as shown by cellular imaging, and has unprecedented near-IR light photocytotoxicity in different cancer cells.

The complex [FeL(cat)(NO_3)] (**1**, Figure 1) was synthesized in approximately 85% yield from the reaction of $Fe(NO_3)_3{\cdot}9H_2O$ with 9-[(2,2′-dipicolylamino)methyl]anthracene (L) in a 3:2 (v/v) ethanol/acetone mixture, with subsequent addition of catechol (H_2cat) and triethylamine. The product was isolated as a dark violet solid. The complex was characterized by elemental analysis, ESI-MS, and UV/vis spectroscopy (see Table S1 in the Supporting Information). The UV/vis spectrum of **1** in 5% DMF/Tris-HCl buffer (pH 7.2) has two visible bands at 495 and 805 nm. The spectral bands are attributed to the catecholate–iron(III) LMCT transition, which involves two different catecholate frontier orbitals and the dπ* orbital of iron(III) (Figure 1).[19] Complex **1** is a 1:1 electrolyte in DMF with a Λ_M value of 71 $S\,m^2\,M^{-1}$, which suggests dissociation of the nitrate ligand. The ESI mass spectrum of **1** in MeOH has a single mass peak at $m/z = 553.33$, which corresponds to $[M-(NO_3)]^+$ (Figure S1 in the Supporting Information). Complex **1** in aqueous methanol, however, has an additional peak at $m/z = 571.27$, which is assignable to $[M-(NO_3)+(H_2O)]^+$. The peak shifted

[*] U. Basu, A. Hussain, Prof. A. R. Chakravarty
Department of Inorganic and Physical Chemistry
Indian Institute of Science, Bangalore, Karnataka (India)
E-mail: arc@ipc.iisc.ernet.in
I. Khan, Prof. P. Kondaiah
Department of Molecular Reproduction, Development and Genetics
Indian Institute of Science, Bangalore, Karnataka (India)
E-mail: paturu@mrdg.iisc.ernet.in

[**] We thank the Department of Science and Technology (DST), Government of India, for financial support (SR/S5/MBD-02/2007) and the Alexander von Humboldt Foundation (Germany) for an electrochemical system. A.R.C. thanks DST for a J. C. Bose Fellowship. I.K and A.H. thank the Council of Scientific and Industrial Research (CSIR), New Delhi, for research fellowships. We thank Prof. Sudhakar Rao and Mr. Saravanan, Civil Engineering Department, IISc for the AAS facility.

Supporting information for this article is available on the WWW under http://dx.doi.org/10.1002/anie.201108360.

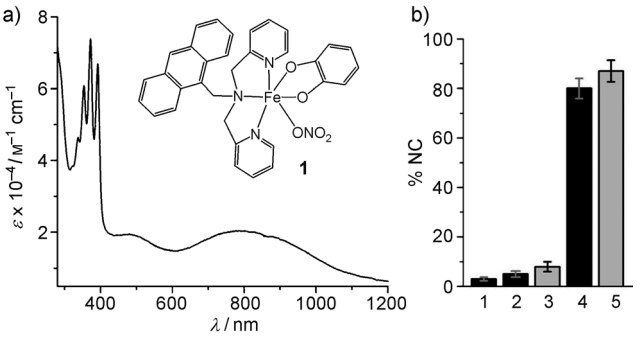

Figure 1. a) UV/vis spectrum of **1** recorded in 5% DMF/Tris-HCl buffer (pH 7.2). b) Photocleavage of pUC19 DNA (30 μM) by L (25 μM in 5%DMF/Tris buffer) and **1** (25 μM in 5% DMF/Tris buffer) in red light at 785 nm (bars 1, 2 and 4) and 633 nm (bars 3 and 5). 1 = DNA control; 2 = L; 3 = L; 4 = **1**; 5 = **1**.

by two units when D_2O was used instead of water to give the additional peak at $m/z = 573.33$. The ESI mass spectrum and conductivity data suggest the presence of [{FeL(cat)(H_2O)}-(NO_3)] as a stable species in the aqueous phase. The magnetic moment of the complex in the solid state is 5.85 μ_B, which suggests a $t_{2g}^3e_g^2$ electronic configuration for the iron(III) center. The IR spectrum of **1** has a characteristic peak for the metal-bound NO_3^- ligand (Figure S2 in the Supporting Information). The complex undergoes an irreversible Fe^{III}/Fe^{II} redox process near −0.4 V (versus saturated calomel electrode) in DMF-0.1M TBAP, and a quasireversible redox response at 0.39 V from a catechol/semiquinone radical species (Figure S3 in the Supporting Information).[20] Complex **1** has an emission band at 420 nm in DMSO upon excitation at 370 nm, and has a quantum yield value of 0.035 (Figure S4 in the Supporting Information).

Complex **1** was structurally characterized by single-crystal X-ray diffraction. The complex crystallized in a $P\bar{1}$ space group in triclinic crystal system (Tables S2 and S3 and Figure S4 in the Supporting Information; CCDC 853997 contains the supplementary crystallographic data for this paper. These data can be obtained free of charge from The Cambridge Crystallographic Data Centre via www.ccdc.cam.ac.uk/data_request/cif). The molecular structure reveals a distorted octahedral geometry that has an FeN_3O_3 core with L and dianionic 1,2-dihydroxybenzene (catecholate) showing facially binding tridentate and bidentate co-ordination modes, respectively (Figure 2). The sixth coordination site is occupied by a nitrate group that is bonded through one of the oxygen atoms. The pendant anthracenyl moiety is unencumbered and could bind to DNA. The Fe(1)−$O(1)_{nitrate}$ distance is 2.023(3) Å. This is significantly longer than the other two Fe−O catecholate distances (1.922(2) Å and 1.954(2) Å). The Fe(1)-N(1) distance *trans* to the Fe(1)-O(1) bond is longer (2.229(3) Å) than the Fe(1)-N(2) and Fe(1)-N(3) distances (2.179(3) Å and 2.156(3) Å). The dissociation of the nitrate group could generate a distorted square-pyramidal structure with an Fe(1)-O(2)-O(3)-N(2)-N(3) base that has an elongated Fe(1)−N(1) axial bond. The complex in an aqueous solution exists as an aqua adduct.

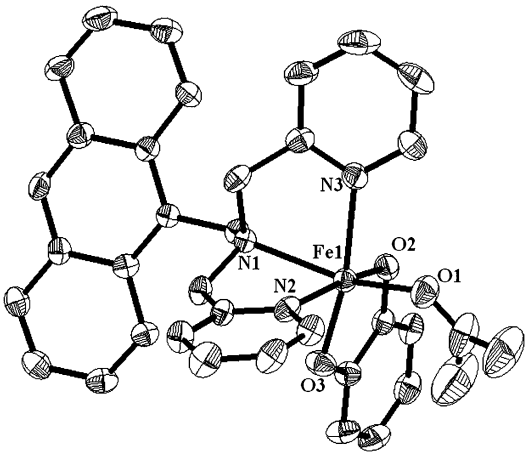

Figure 2. An ORTEP view of [FeL(cat)(NO_3)] with ellipsoids at 50% probability level. The hydrogen atoms are omitted for clarity.

The stability of the core that is coordinated to the L and cat ligands was investigated by spectral and electrochemical methods in DMSO. The complex in 50% aqueous DMSO or DMEM/10% fetal bovine serum (FBS) medium did not show any change in the position or in the intensity of the UV/vis absorption band after 24 h (Figure S6 in the Supporting Information). Time-dependent voltammetric scans of the Fe^{III}/Fe^{II} redox couple did not show any change in the redox response up to 24 h (Figure S6 in the Supporting Information).

The binding of **1** to calf thymus DNA (ct-DNA) was investigated by UV/vis spectral absorption in Tris-HCl buffer (pH 7.2), DNA thermal denaturation in phosphate buffer (pH 6.8), and viscosity measurements (Figure S7 in the Supporting Information). The intrinsic DNA binding constant (K_b) of **1** is $(1.5 \pm 0.1) \times 10^5 M^{-1}$. A 4.8 °C ΔT_m value for **1** suggests partial intercalation of the complex into ct-DNA. Complex **1** caused a significant increase in the relative specific viscosity relative to the DNA groove-binding Hoechst dye, but less than that of the DNA intercalator ethidium bromide (EB). The ΔT_m value and the viscosity data suggest that the mode of binding of **1** to ct-DNA is partial intercalative.

The DNA photocleavage potential of **1** in red light was studied by using supercoiled (SC) pUC19 DNA. The photocytotoxicity of **1** was studied in various cancer cell lines. The mode of cell death was studied through the fragmentation of genomic DNA and by an Annexin-V/PI binding assay. 2′,7′-dichlorodihydrofluorescein diacetate (DCFDA) assay was carried out to study the generation of reactive oxygen species (ROS). Mechanistic studies were done with the ROS quencher *N*-acetyl cysteine (NAC). DNA photocleavage experiments with a diode laser at 785 nm (100 mW) and a HeNe laser at 633 nm (12 mW) showed approximately 85% conversion of the SC DNA to its nicked circular (NC) form at a concentration of 25 μM of complex (Figure 1b, see also Figure S8 in the Supporting Information).

Complex **1** did not cause any apparent DNA cleavage in the dark or in the presence of external oxidizing (H_2O_2) or reducing (glutathione, GSH) agents (Figure S9 in the Supporting Information). The ligands or the metal salt alone did not cause any significant DNA photocleavage activity in red light. The photocleavage of DNA proceeds by a hydroxyl radical pathway. Singlet oxygen quenchers, for example, 2,2,6,6-tetramethyl-4-piperidone (TEMP), 1,4-diazabicyclo-[2.2.2]octane (DABCO), and NaN_3 did not inhibit the DNA photocleavage reaction, whereas the use of hydroxyl radical scavengers (DMSO, KI, catalase) and superoxide radical scavengers (superoxide dismutase, SOD) inhibited the DNA photocleavage activity significantly (Figure S10 in the Supporting Information). The detection of insignificant chemical nuclease activity and remarkable DNA photocleavage activity in near-IR light at 785 nm led us to investigate the photodynamic effect of **1** in different cancer cells.

The photocytotoxic behavior of **1** was studied by using an 3-(4,5-dimethylthiazole-2-yl)-2,5-diphenyltetrazolium bromide (MTT) assay in human cervical carcinoma (HeLa) and breast cancer cells (MCF-7). The IC_{50} values were (6.2 ± 0.1) μM in HeLa cells and (11.3 ± 0.1) μM in MCF-7 cells, when irradiated with light in the 400-700 nm wavelength

range (Luzchem photoreactor, 10 J cm^{-2}, Figure 3a, see also Figure S11 in the Supporting Information). The IC_{50} value was above 100 μM in the dark for both the cell lines. The

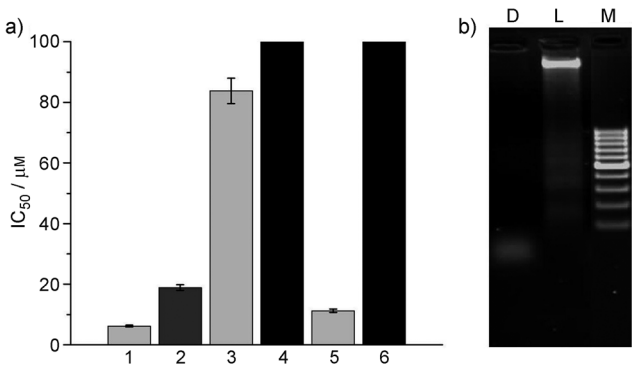

Figure 3. a) Photocytotoxicity of **1** in HeLa (bars 1–4) and MCF-7 cancer cells (bars 5 and 6) after 4 h incubation in the dark (bars 4 and 6) and after photoirradiation with visible light (400–700 nm, 10 J cm^{-2}, bars 1, 3, and 5) or red light (600–720 nm, 50 J cm^{-2}, bar 2). Bar 3 = photocytotoxicity of **1** after irradiation in the presence of NAC. b) DNA ladder of **1** in HeLa cells that shows apoptosis (D = dark, L = light, M = Marker 100 bp).

IC_{50} value was (2.9 ± 0.2) μM when the HeLa cells were irradiated without removing the complex from the medium. Low dark toxicity and significant photocytotoxicity of **1** are indeed remarkable and warranted further studies. As PDT uses red light, we studied the photocytotoxicity of **1** in cells on a biomedical instrument (Waldmann PDT 1200 L 600–720 nm, 50 J cm^{-2}) which is used for the treatment of dermatological cancer or lesions. The photocytotoxicity of **1** in HeLa cells was found to be approximately five times higher than that in the dark, which gave an IC_{50} value of 18.8 μM with this light source. A comparison of the IC_{50} values of **1** with other compounds is made in Table 1.[21,22] Complex **1** has similar photocytotoxicity to that reported for Photofrin, but with significantly less dark toxicity. The dark toxicity of **1** in HeLa cells is less than that of the bleomycin mimic iron(II) complex $[Fe(Phqpy)]^{2+}$ (IC_{50} = 7.7 μM in the dark) and cisplatin.

Complex **1** was tested to ascertain the mode of cell death by analyzing the fragmentation of genomic DNA. A DNA ladder was detected in HeLa cells on treatment with **1** and photoirradiation (400–700 nm, 10 J cm^{-2}, Figure 3b). However, no such DNA ladder was evident when the cells were treated with **1** in the dark, which indicates that the death of the cells is photoinduced by an apoptotic pathway. The Annexin-V/PI binding assay also suggests cell death by an apoptotic pathway. A 4 h incubation of the cells with **1** and subsequent irradiation with light (400–700 nm, 10 J cm^{-2}) caused approximately 25% of the cells to undergo early apoptosis, and only approximately 4% of the cells had necrotic damage (Figure S12 in the Supporting Information).

We examined the generation of ROS by using a DCFDA assay. DCFDA is a cell permeable fluorogenic probe which undergoes oxidation to form 2′,7′-dichlorofluorescein (DCF), which has an emission maximum at 528 nm. The fluorescence of DCF was detected and quantified by fluorescence-activated cell sorting (FACS). H_2O_2, which rapidly oxidizes DCFDA, was used as the positive control and has a maximum shift in the emission band that corresponds to maximum production of DCF. The cells that were treated with **1** and DCFDA in the dark did not show any formation of DCF. However, on exposure to light the cells produced DCF as shown by the shift in the emission band, which is close to that of the H_2O_2 band. To further confirm the role of ROS in cell death, we incubated the HeLa cells with **1** and treated them with NAC after irradiation. These cells did not show any significant formation of DCF. The IC_{50} value of the complex after irradiation increased 15-fold when pretreated with NAC (Column 3 in Figure 3a, see also Figure S13 in the Supporting Information). It is thus affirmed that the photocytotoxicity of **1** is reduced as a result of a decrease in the generation of ROS in presence of NAC.

The uptake of **1** into HeLa cells as a function of time was investigated by using a laser scanning confocal microscope. Images were recorded after incubating the cells with **1** for 2 h and 4 h. The dual staining with **1** and propidium iodide (PI) showed that in 2 h a significant fraction of **1** was taken up by the nucleus, as can be seen in the merged image shown in Figure 4c. After 4 h there was hardly any change and the cells showed almost complete accumulation of **1** in the nucleus

Table 1: IC_{50} values of two iron complexes, Photofrin and cisplatin in HeLa and MCF-7 cell lines.

Compound	IC_{50} [μM] HeLa		MCF-7	
	Light	Dark	Light	Dark
1[a]	(6.2±0.1)[b]	>100	(11.3±0.1)	>100
$[Fe^{II}(Phqpy)]^{2+}$[c]		(7.7±0.1)		(68.5±0.2)
Photofrin[d]	(4.3±0.2)	>41		
Cisplatin[c]		(20.5±0.2)		(78.2±0.2)

[a] The IC_{50} values are in visible light (400–700 nm). [b] The IC_{50} value is (18.8 ± 0.1) in red light (600–720 nm, 50 J cm^{-2}). [c] Values taken from Ref. [21]. Phqpy = 2,2′:6′,2″:6″,2‴:6‴,2⁗-phenylquinquepyridine. [d] Values taken from Ref. [22].

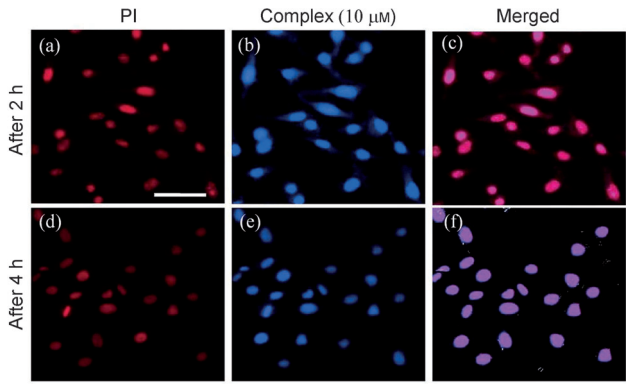

Figure 4. Confocal images of **1** (10 μM) in HeLa cells after 2 h (a–c) and 4 h (d–f) showing cellular uptake. Panels (a) and (d) show the red fluorescence of PI. Panels (b) and (e) show the fluorescence of **1**. Panels (c) and (f) show the merged images of the fluorescence of PI and **1**. Scale bar = 18 μm.

(Figure 4 f). The uptake of **1** into the HeLa cells was quantified by using atomic absorption spectroscopy (AAS). We estimated the total iron content in the cell lysate after incubating the cells with **1** for 4 h and compared it with the same from untreated cells. There was a threefold increase in the quantity of iron in cells that were treated with **1** relative to the untreated cells (Figure S14 in the Supporting Information).

In conclusion, the iron(III) complex **1**, which has an anthracenyl moiety as photosensitizer, fluorophore, and intercalative DNA binder, a catecholate ligand for the near-IR-light LMCT band, and iron as a bioessential metal is an effective photocytotoxic agent that has significant nuclear uptake and causes photoinduced apoptotic cell death in near-IR light. Further studies to explore the effectiveness of **1** in other cancerous cell lines are in progress to explore its efficacy in photodynamic therapy. Complex **1** with its negligible dark toxicity and significant near-IR-light photocytotoxicity is distinctly different from other metal-based PDT agents and its activity compares well with the clinically approved PDT drug Photofrin.

Received: November 28, 2011
Revised: January 16, 2012
Published online: January 30, 2012

Keywords: antitumor agents · bioinorganic chemistry · cancer · iron · photodynamic therapy

[1] N. J. Farrer, L. Salassa, P. J. Sadler, *Dalton Trans.* **2009**, 10690 – 10701.
[2] U. Schatzschneider, *Eur. J. Inorg. Chem.* **2010**, 1451 – 1467.
[3] H. T. Chifotides, K. R. Dunbar, *Acc. Chem. Res.* **2005**, *38*, 146 – 156.
[4] a) N. L. Fry, P. K. Mascharak, *Acc. Chem. Res.* **2011**, *44*, 289 – 298; b) A. D. Ostrowski, P. C. Ford, *Dalton Trans.* **2009**, 10660 – 10669.
[5] R. Bonnett, *Chemical Aspects of Photodynamic Therapy*, Gordon & Breach, London, UK, **2000**.
[6] J. L. Sessler, R. A. Miller, *Biochem. Pharmacol.* **2000**, *59*, 733 – 739.
[7] J. P. Celli, B. Q. Spring, I. Rizvi, C. L. Evans, K. S. Samkoe, S. Verma, B. W. Pogue, T. Hasan, *Chem. Rev.* **2010**, *110*, 2795 – 2838.
[8] K. Szacilowski, W. Macyk, A. Drezewiecka-Matuszek, M. Brindell, G. Stochel, *Chem. Rev.* **2005**, *105*, 2647 – 2694.
[9] C. J. Burrows, J. G. Muller, *Chem. Rev.* **1998**, *98*, 1109 – 1152.
[10] S. I. Moriwaki, J. Misawa, Y. Yoshinari, I. Yamada, M. Takigawa, Y. Tokura, *Photodermatol. Photoimmunol. Photomed.* **2001**, *17*, 241 – 243.
[11] a) N. J. Farrer, J. A. Woods, L. Salassa, Y. Zhao, K. S. Robinson, G. Clarkson, F. S. Mackay, P. J. Sadler, *Angew. Chem.* **2010**, *122*, 9089 – 9092; *Angew. Chem. Int. Ed.* **2010**, *49*, 8905 – 8908; b) F. S. Mackay, J. A. Woods, P. Heringová, J. Kašpárková, A. M. Pizarro, S. A. Moggach, S. Parsons, V. Brabec, P. J. Sadler, *Proc. Natl. Acad. Sci. USA* **2007**, *104*, 20743 – 20748.
[12] A. M. Angeles-Boza, H. T. Chifotides, J. D. Aguirre, A. Chouai, P. K. L. Fu, K. R. Dunbar, C. Turro, *J. Med. Chem.* **2006**, *49*, 6841 – 6847.
[13] a) P. C. Ford, *J. Am. Chem. Soc.* **2009**, *131*, 15963 – 15964; b) A. A. Eroy-Reveles, Y. Leung, C. M. Beavers, M. M. Olmstead, P. K. Mascharak, *J. Am. Chem. Soc.* **2008**, *130*, 6650 – 6650.
[14] T. Köpke, M. Pink, J. M. Zaleski, *Chem. Commun.* **2006**, 4940 – 4942.
[15] R. J. Ernst, H. Song, J. K. Barton, *J. Am. Chem. Soc.* **2009**, *131*, 2359 – 2366.
[16] J. Wang, S. L. H. Higgins, B. S. J. Winkel, K. J. Brewer, *Chem. Commun.* **2011**, *47*, 9786 – 9788.
[17] a) B. Maity, M. Roy, B. Banik, R. Majumdar, R. R. Dighe, A. R. Chakravarty, *Organometallics* **2010**, *29*, 3632 – 3641; b) P. K. Sasmal, S. Saha, R. Majumdar, R. R. Dighe, A. R. Chakravarty, *Chem. Commun.* **2009**, 1703 – 1705; c) S. Saha, R. Majumdar, M. Roy, R. R. Dighe, A. R. Chakravarty, *Inorg. Chem.* **2009**, *48*, 2652 – 2663.
[18] a) K. Visvaganesan, R. Mayilmurugan, E. Suresh, M. Palaniandavar, *Inorg. Chem.* **2007**, *46*, 10294 – 10306; b) P. U. Maheswari, S. Roy, H. den Dulk, S. Barends, G. van Wezel, B. Kozlevcar, P. Gamez, J. Reedijk, *J. Am. Chem. Soc.* **2006**, *128*, 710 – 711.
[19] P. C. A. Bruijnincx, M. Lutz, A. L. Spek, W. R. Hagen, G. van Koten, R. J. M. K. Gebbink, *Inorg. Chem.* **2007**, *46*, 8391 – 8402.
[20] N. Anitha, M. Palaniandavar, *Dalton Trans.* **2011**, *40*, 1888 – 1906.
[21] E. L. M. Wong, G. S. Fang, C. M. Chi, N. Zhu, *Chem. Commun.* **2005**, 4578 – 4580.
[22] E. Delaey, F. Van Laar, D. De Vos, A. Kamuhabwa, P. Jacobs, P. De Witte, *J. Photochem. Photobiol. B* **2000**, *55*, 27 – 36.

